

A CASE OF COMPRESSION FAILURE IN CONCRETE DUE TO STRESS RELEASE

P. Stroeven,
Faculty of Civil Engineering, Delft University of Technology, Delft
The Netherlands

Abstract

Experimental investigations in the field of low-cycle compression fatigue at a relatively high upper loading have revealed a drop in life time under certain loading conditions relevant for off-shore constructions. The prevailing mechanism leading to such premature fracture was cracking due to stress release. It occurred at a frequency of 17.5 Hz and at maximum stress amplitude. A structural study based on a stereological analysis of the damage structure at the end of testing offered insight into the damage evolution process under these conditions.

1 Introduction

Mesoscopic cracks will develop in the loading direction in concrete specimens subjected to uniaxial compression because of 'parasitic' tensile stresses. These cracks, when opened up under such (local) tensile stresses, can propagate further in the loading direction upon closing of the crack due to stress release. This is caused by

mismatch of crack surfaces. Under certain low cycle compression fatigue conditions, crack development in a direction *perpendicular* to the loading direction has been monitored earlier (Graf and Brenner, 1939). Though of secondary nature, this mechanism has been demonstrated to sometimes dramatically speed up the process of damage evolution. Compared to the case in which the upper level was similar but the stress amplitude considerably reduced, the number of cycles to fracture was about *one order of magnitude lower* (Kooistra and Frencken, 1975/76)! The loading conditions are relevant for certain off-shore situations, so that a detailed study offering insight into the mechanisms of damage evolution can be considered of practical value. The case of fracture due to stress release is also of fundamental interest because of more recent fracture mechanical developments.

2 Experimental

Extensive testing was performed in low-cycle compression fatigue to evaluate the effects of average stress level, stress amplitude and frequency on the number of cycles to fracture, N . The frequencies covered were 17.5 Hz and 0.175 Hz. The upper stress level, σ'_t , was taken for all tests at 87.5 % of the 28-days short term compressive strength, σ'_{f28} , of prismatic specimens with similar composition. Hence, this is well above the so called endurance limit. A relative stress amplitude, S , is defined by $S = (\sigma'_t - \sigma'_b) / \sigma'_{f28}$, in which σ'_b is the lower stress level. S varied in the investigations between zero and 0.475. Out of the eight stress amplitude cases encompassed in the experiments three were included in the structural study, to be discussed in what follows. The selected cases, $S = 0$, $S = 0.075$ and $S = 0.35$, represent the mechanical states of permanent loading, and of low-cycle fatigue loading with small, respectively, with large load amplitude.

A total number of 72 prismatic specimens ($100 \times 100 \times 345 \text{ mm}^3$) were casted from concrete with a maximum grain size of 8 mm and a water to cement ratio of 0.46. Average 28-days compressive strength of reference prisms amounted to 56.2 MPa. The low-cycle fatigue prisms were stored 10 days under water, followed by 7 days under climatized conditions (22°C , 50%RH), whereupon the specimens were placed until the day of testing at about 1 month in the test room. Sieve curves were between the A₈ and B₈ curves of DIN 1045. A single specimen whose deformational behaviour was as close as possible to that of the group average was selected from the 5 to 16 similarly tested specimens. The deformations were

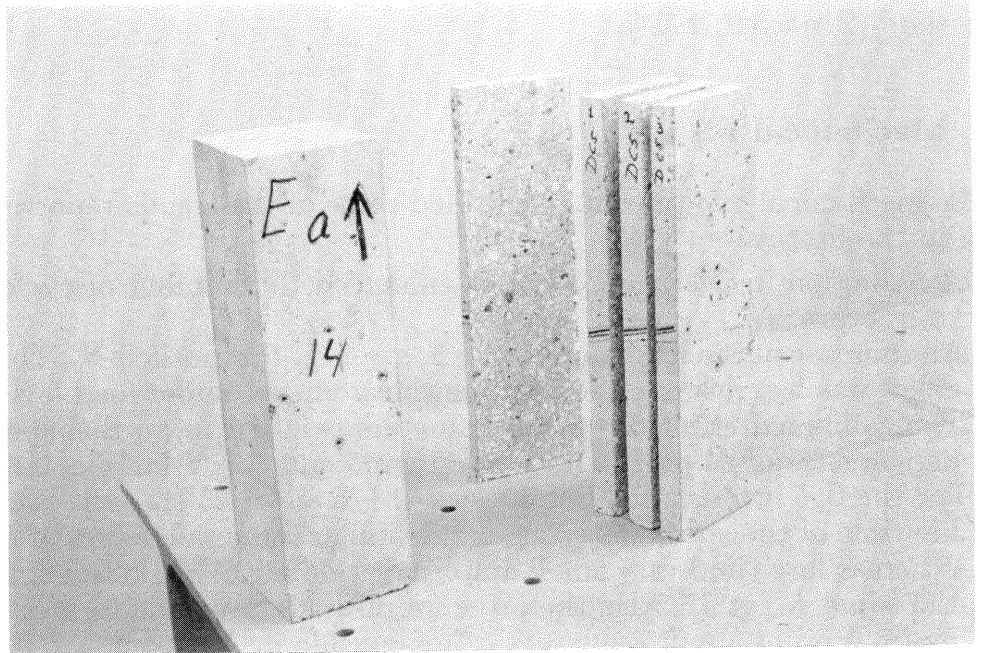


Fig. 1. Specimens subjected to serial sectioning for the stereological analysis

recorded by clip gauges in longitudinal and transverse directions. Specimens were subjected to a sinusoidally varying load in a servohydraulic testing machine. The loading process was automatically stopped when the transverse deformation attained a certain threshold value (Reinhardt, et al, 1978). This rendered possible to study the internal damage structure of the specimens without introducing a significant bias in the number of cycles to fracture.

Each selected specimen was axially sliced to yield three equally spaced sections at a distance of 27 mm as shown in Fig. 1. The specimens were casted, compacted and stored in vertical position. Since the loading was applied also in the same direction, the longitudinal axis of the specimen can be considered an axis of symmetry of the damage structure (excluding boundary zones). Fields of $51 \times 102 \text{ mm}^2$ were selected at the center of each section image. Hence, a sample encompassed three independent so called "vertical" fields. These could be probed by directed secants to provide zero-dimensional information (intersections points), which could be transformed by stereological notions into three-dimensional global damage data. The distance between the grid lines was optimized to yield a number of intersections roughly equal to the number of cracks in a field. In doing so, a total test line length of 1734 mm was obtained. Contrast was improved by employing the filtered particle

method (Stroeven, 1979a).

3 Mechanical results

The mechanical experiments confirmed some of the trends reported on in the literature

- A reduction in average load level enhanced the number of cycles to fracture, N .
- An increase in the load amplitude, S , strongly diminished N . This effect was less dramatic for a somewhat reduced upper load level.
- The combined effect of both parameters resulted in an S-shaped dependence of N on S with a maximum value of N for $S \simeq 0.8$.
- For the two investigated frequencies (0.175 and 17.5 Hz), the total life time of the specimens was found similar for small values of S .
- Whereas large and very small amplitudes led at 0.175 Hz to about the same N , at 17.5 Hz the large amplitudes gave rise to a dramatic drop of about one order of magnitude in N .
- Longitudinal, transverse, and volumetric strains, and hence Poisson's ratio, developed linearly over most of the test period; the non-linear part close to the end of the test was most pronounced for the intermediate amplitude case and absent for the highest one.
- Transverse deformational capacity was optimum for the intermediate amplitude case.
- Longitudinal strains at fracture were proportional to S , confirming results of Awad and Hilsdorf (1974).

Since a more extensive discussion of these data is not the subject of this paper, one is referred to the relevant literature (Kooistra and Vrencken, 1975/76; Reinhardt, et al, 1978; Stroeven, 1978; Stroeven, 1979b). In this paper, attention will primarily focus on the dramatic drop in life time under higher amplitudes at 17.5 Hz.

4 Stereological methodology

A partially linear system, as a close approximation for the actual damage structure, can be emphasized as a mixture of 3-D and 1-D systems. The cracks are in both systems randomly distributed as to location. In the first case, the cracks are also randomly distributed as to orientation, whereas in the second one all cracks are parallel to a line, the axis of the specimen. In a vertical section, the 3-D system gives rise to a random pattern of traces, while the 1-D system

leads to traces parallel to the axis of the specimen. The number of intersections with a parallel line probe is indicated by P , and its density by $P/L = P_L$. Perpendicular to the orientation axis of the traces the intersection density will be maximum, while a minimum is found in the orthogonal direction. It is well-known that the intersection density in a certain direction, $P_L(\theta)$ is an unbiased estimator of the total projected length of the traces, per unit of area, on a line perpendicular to the grid direction, $L'_A(\theta + \frac{\pi}{2})$ (Stroeven, 1979a). Hence,

$$P_L(\theta) = E[L'_A(\theta + \frac{\pi}{2})] \quad (1)$$

For the axial and transverse direction it is readily found that

$$P_L(0) = E[\frac{2}{\pi}L_{A3}] \quad (2)$$

$$P_L(\frac{\pi}{2}) = E[\frac{2}{\pi}L_{A3} + L_{A1}] \quad (3)$$

where L_{A1} and L_{A3} are the areal trace density in the 1-D and 3-D system, respectively. Obviously, $L_A = L_{A1} + L_{A3}$, so that

$$P_L(\frac{\pi}{2}) + (\frac{\pi}{2} - 1)P_L(0) = E[L_A] \quad (4)$$

The degree of orientation in the trace pattern can be defined by

$$\omega_2 = \frac{L_{A1}}{L_A} \quad (5)$$

which upon substitution of the trace density components in eqs (2) to (4) leads to

$$\frac{P_L(\frac{\pi}{2}) - P_L(0)}{P_L(\frac{\pi}{2}) + (\frac{\pi}{2} - 1)P_L(0)} = E[\omega_2] \quad (6)$$

The assumption of a partially linear crack structure implies that the rose of the number of intersections in the image plane has main axes given by eqs (2) and (3) and the intermediate radii are governed by

$$P_L(\theta) = \frac{2}{\pi}L_{A3} + L_{A1} \sin \theta = P_L(0) + [P_L(\frac{\pi}{2}) - P_L(0)] \sin \theta \quad (7)$$

The 3-D interpretation of a similar set of observations is equally simple! The same probabilistic principle holds. Hence

$$P_L(0) = E[\frac{1}{2}S_{V3}] \quad (8)$$

$$P_L(\frac{\pi}{2}) = E[\frac{1}{2}S_{V3} + \frac{2}{\pi}S_{V1}] \quad (9)$$

In analogy with eq (4) S_V is given by

$$\frac{\pi}{2}P_L\left(\frac{\pi}{2}\right) + \left(2 - \frac{\pi}{2}\right)P_L(0) = E[S_V] \quad (10)$$

The degree of spatial orientation $\omega_3 = S_{V1}/S_V$ is found upon substitution of the relevant specific crack surface areas in eqs (8) to (10)

$$\frac{\frac{\pi}{2}[P_L\left(\frac{\pi}{2}\right) - P_L(0)]}{\frac{\pi}{2}P_L\left(\frac{\pi}{2}\right) + \left(2 - \frac{\pi}{2}\right)P_L(0)} = E[\omega_3] \quad (11)$$

The number of crack traces per unit of area, N_A , and their 2-D size distribution can be determined with the help of an automatic image analyser (in the present case a Quantimet 720). Although the latter can only be an approximation because of interpretation difficulties with branching cracks, the differences in distribution curves for various amplitudes were significant. The area scanned in this case amounted to 1429 mm².

5 Structural results

With growing amplitudes ($S = 0, 0.075$ and 0.35) the stereological analyses revealed

- the crack extension (i.e. L_A and S_V) to steadily increase.
- the number of cracks (N_A) to be significantly smaller for the intermediate amplitude.
- the average crack length (i.e. $\bar{x} = L_A/N_A$) to have its maximum value for the intermediate amplitude.
- the crack size distribution curve of the intermediate amplitude to encompass a relatively small number of tiny cracks.
- the main direction of orientation of the cracks to change from axial into transverse for the largest amplitude case.
- the degree of orientation to initially increase but to steeply decline for the largest amplitude case.

6 Damage evolution due to stress release

A reduction in lower load level to below the onset of structural loosening gives rise to a destructive effect of the amplitude. The time to fracture is thereby dramatically shortened and the damage evolution rate enormously increased. The latter is even more striking, since

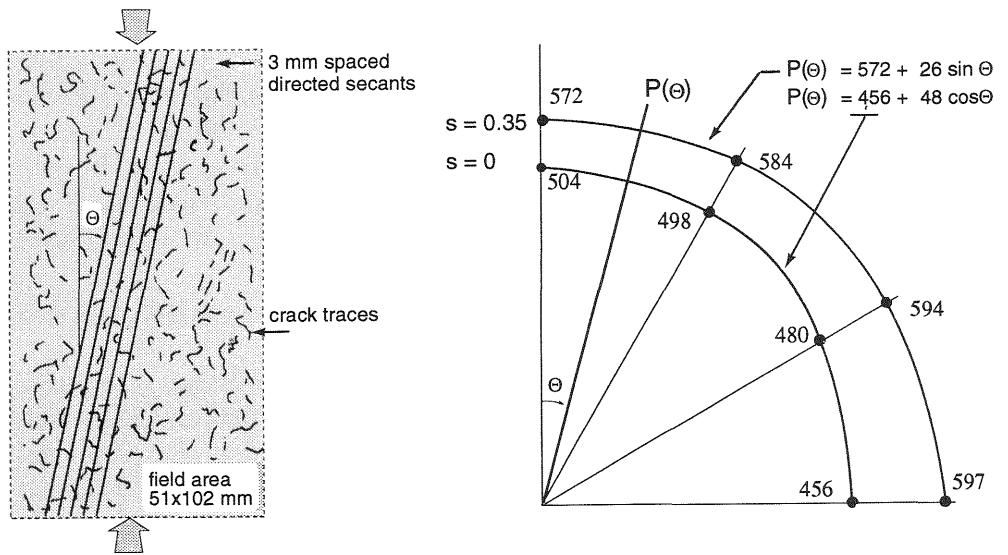


Fig. 2. Roses of intersections of crack patterns in vertical sections of prisms subjected to low-cycle fatigue pertaining to the cases $S = 0$ and $S = 0.35$

specific crack surface area (S_V) is enlarged by 27.2% as a result of the amplitude effect! The short life time at large amplitude loading allows the origination of a large number of tiny cracks in both axial and transverse directions. A similar average crack length of about 3.5 mm in the extreme cases also points toward a small extent of crack coalescence under higher amplitudes. Transverse cracking is clearly revealed by the roses of intersections (Fig. 2). The value of $P_L(\frac{\pi}{2})$ is increased by 13.5% upon reduction of the lower load level to about 50% of the 28-days short time compressive strength of the material (i.e. $S = 0.35$). Over the same range, $P_L(0)$ is increased by 30.9% (coefficient of variation is only 3 to 4% (Stroeven, 1978))! Neither of the systems of tiny cracks can give rise to significant inelastic deformations, so that the strain-time curves are linear. The 'impact' effect of load release on mesolevel at 17.5 Hz is absent at the lower frequency of 0.175 Hz, preventing crack development in the orthogonal direction.

The micromechanical explanation was given earlier. Vile (1965) already pointed toward the crucial place the river aggregate constitutes in the damage evolution process under steadily increasing compressive loadings. Stroeven has further detailed this model for mesocracking by detailed microscopical studies of cracking in which contrast was improved by the filtered particle method (Forrester, 1965; Stroeven, 1973). The debris found by various investigators after ultimate loading in compression confirmed the model charac-

teristics (Newman and Newman, 1969; Stroeven, 1973; Perry and Gillott, 1977): gravel and sand particles were found to have only partly debonded from the matrix; two mortar 'cones' were still fixed in a symmetrical position to the particles. The low bond strength at particle-matrix interface was shown by Wittmann, long before the attention started to focus on the interfacial transition zone, to be due to imperfect packing, thus strongly limiting van der Waals forces (Wittmann, 1971).

Because of an increasingly unfavourable local stress state, the axially oriented bond crack has to leave the interface. The formation of so called en échelon tensile crack arrays at these locations, in analogy with findings in rock mechanical research (Gramberg, 1970) was confirmed by Stroeven (1973). They weaken in an oblique direction the mortar matrix, facilitating secondary shear fracture along these zones. By nature of their origination these slip planes are relatively rough, so that to a certain extent under stress release the restoration of the material body will be resisted. This will be more pronounced under lower release rates, of course. Since the upper loading in the present experiments is well beyond the so called onset of structural loosening or crack initiation strength, damage evolution has proceeded into this stage of oblique shear cracking. When the lower load level will be below the crack initiation strength, the oblique slip planes will be subjected to reversed shear forces to enforce the restoration of the material body. This however induces axial tensile stresses in the loading direction of the mesoscopic elements which were created by particle-matrix debonding and succeeding slip along the en échelon crack zones (Fig. 3). As a result debonding may occur between the conical deposits and the particles, leading to the system of secondary cracks under stress release.

7 Conclusions

Damage is a fractal-like phenomenon. Hence, observations on damage evolution are resolution-dependent. This also holds for the present experiments. Extent of damage and characteristics of the crack orientation distribution are a function of the magnification set by the researcher (in the present case all cracks exceeding about 0.2 mm in length were considered). The data presented herein nevertheless reveal qualitative structural differences between loading regimes, which allow to gain a clear insight into the operative damage evolution mechanisms. This has practical implications for the design of concrete constructions in situations where larger load amplitudes may occur at higher frequencies in the low-cyclic loading

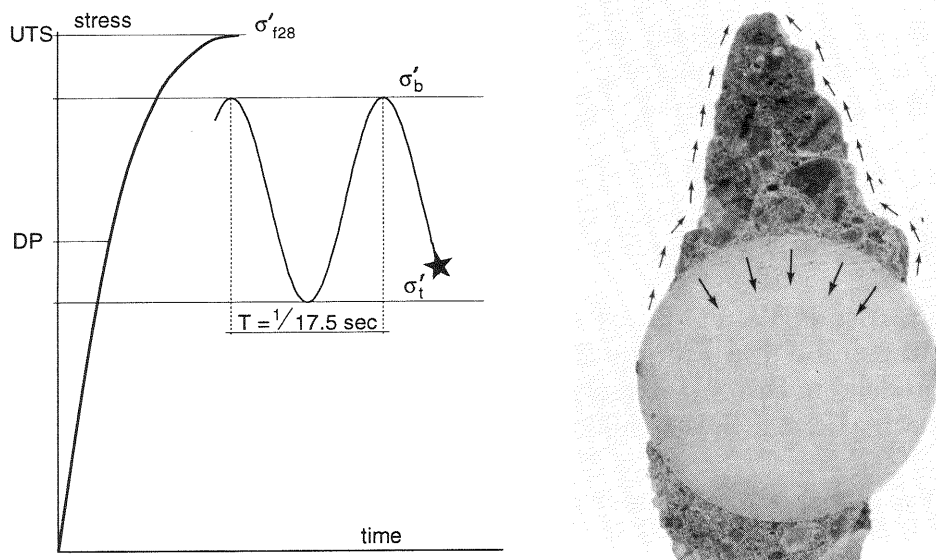


Fig. 3. Model for crack development under stress release in the compression domain

domain. The practical significance of the phenomenon of cracking due to stress release will diminish with declining value of the upper load level. Nevertheless, the phenomenon has its intrinsic scientific value when seen in the light of modern applications of fracture mechanics to concrete.

8 References

- Awad, M.E., Hilsdorf, H.K. (1974) Strength and deformation characteristics of plain concrete subjected to high compressive repeated and sustained loads, in **Fatigue of concrete**. ACI Spec. Publ. SP-41, Detroit, 1-13.
- Forrester, J.A. (1965) Discussion: Propagation of cracks and their detection under short- and long-term loading, in **The Structure of Concrete** (eds A.E. Brooks and K. Newman), Cem. Concr. Ass., London, 157-160.
- Gramberg, J. (1970) Klastische en kataklastische processen en hun betekenis voor de gesteentemechanica. PhD Thesis, Delft Univ. Technology, Delft, The Netherlands.
- Kooistra, T.R., Vrencken, J.H.A.M. (1975/76) Herhaalde belasting van ongewapend beton. MSc Thesis, Fac. Civil Engr., Delft Univ. Technology, Delft, The Netherlands.

- Newman, K., Newman, J.B. (1969) Failure theories and design criteria for plain concrete, in **Proc. Southampton Civ. Engr. Mat. Conf.** (ed M. Te'eni), Wiley, New York, 963-995.
- Perry, C., Gillott, J.E. (1977) The influence of mortar-aggregate bond strength on the behaviour of concrete in uniaxial compression. **Cem. Concr. Res.**, 5, 553-564.
- Reinhardt, H.W. et al. (1978) Einfluss von Schwingbreite, Belastungshöhe und Frequenz auf die Schwingfestigkeit von Beton bei niedrigen Bruchlastweckselzahlen. **Betonw. und Fertigteiltechnik**, 44, 9, 498-503.
- Stroeven, P. (1973) Some aspects of the micromechanics of concrete. PhD Thesis, Delft Univ. Technology, Delft, The Netherlands.
- Stroeven, P. (1978) Amplitude effect on fatigue behaviour of concrete qualitatively evaluated by stereological techniques, in **Sonderbände der Praktischen Metallographie**, 8, 264-272.
- Stroeven, P. (1979a) Geometric probability approach to the examination of microcracking in plain concrete. **J. Mat. Science**, 14, 1141-1151.
- Stroeven, P. (1979b) Mechanics of microcracking in concrete subjected to fatigue loading, in **Mechanical Behaviour of Materials**, Volume 3 (eds K.J. Miller and R.F. Smith), Pergamon Press, Toronto, 141-150.
- Vile, G.W.D. (1965) Behaviour of concrete under simple and combined stresses. PhD Thesis, Univ. London, London.
- Wittmann, F. (1971) Experiments to determine van der Waals forces, in **Structure, Solid Mechanics and Engineering Design** (ed M. Te'eni), Wiley, London, 295-300.